Supporting Information for:

Unraveling the high-performance oxygen-deficient amorphous manganese oxide as

cathode for advanced zinc ion batteries

Mehdi Karbak[a,b], Mariam Baazizi[a,c], Simon Sayah[a], Cecile Autret-Lambert[d], Yann Tison[e],

Herve Martinez[e,f], Tarik Chafik[b], and Fouad Ghamouss[a,c]*

[a.] *Laboratory of Physical-Chemistry of Materials and Electrolytes for Energy (PCM2E), University of Tours, 37200 Tours, France.*
[b.] *Laboratory of Chemical Engineering and Resources Valorization (LGCVR), Faculty of Sciences and Techniques, University Abdelmalek Essaadi, B.P. 416, Tangier 90010, Morocco.*
[c.] *Department of Materials Science, Energy, and Nano-Engineering, Mohamed VI Polytechnic University, Ben Guerir 43150, Morocco.*
[d.] *Materials Research Group, Microelectronics, Acoustics and Nanotechnologies, GREMAN, (UMR 7347), University of Tours, 37200 Tours, France*
[e.] *Université de Pau et des Pays de l'Adour, E2S UPPA, CNRS, IPREM, Pau, France*
[f.] *Centrale Casablanca, Centre de Recherche Systèmes Complexes et Interaction, Bouskoura 27182, Morocco*

Materials and methods

Materials

Potassium permanganate ($KMnO_4$, AR, $\geq 99\%$), absolute ethanol (C_2H_5OH, $\geq 99.5\%$) and sodium borohydride ($NaBH_4$, $\geq 98.0\%$) were all purchased from SIGMA ALDRICH. All reagents were used as received without any further treatment.
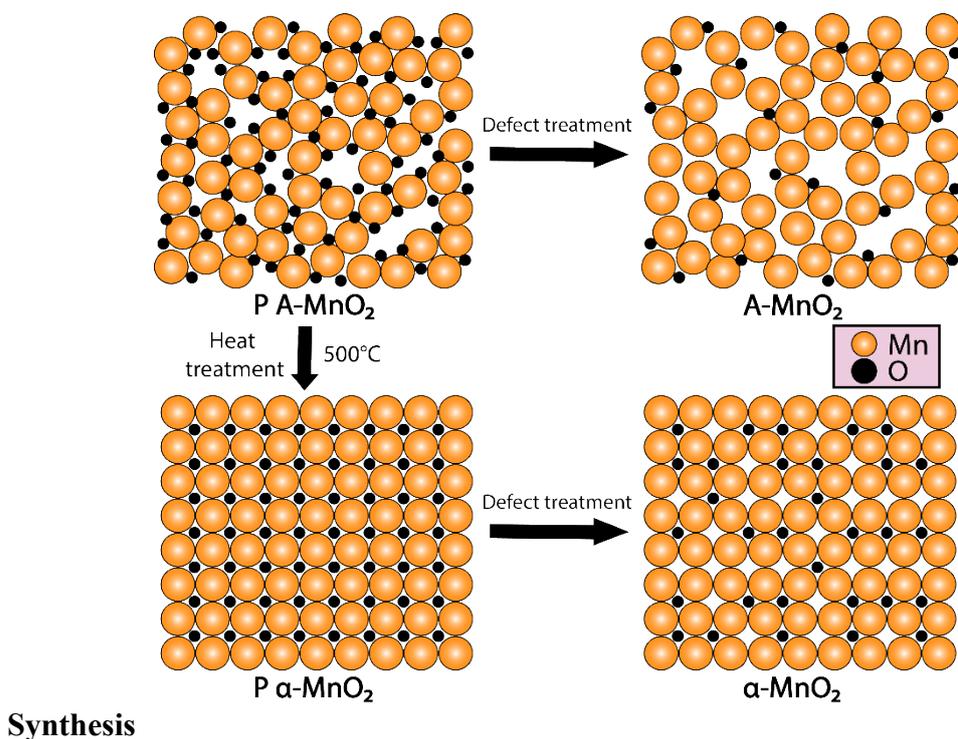
Figure S1: Schematic illustration of the material synthesis

Synthesis

1g of $KMnO_4$ was dissolved in 50 ml of distilled water with vigorous stirring at room temperature followed by adding 100 ml of absolute ethanol. After 2 hours of stirring, a brown precipitate was acquired. The precipitate was filtered and washed with distilled water until the pH of the filtrate equaled 7. Then the resulted material was vacuum-dried at 60°C overnight to form a pristine amorphous MnO_2 (P A-MnO_2). The latter was ground by an agate mortar and calcined under air at 500°C for 2h. The calcined material is named P α-MnO_2. Subsequently, both materials went through an oxygen deficiency treatment previously reported by Junmin

Xue et al.[1] Basically, 1g of the synthesized P MnO_2 was dispersed in 100 ml distilled water. Afterward, 50 ml of 0.1 M $NaBH_4$ solution was prepared and added dropwise to the MnO_2 dispersion. The mixture was stirred for 1 hour and left still for an extra hour. Hence, A-MnO_2 and α-MnO_2 were obtained.

Methods

Morphologies of all samples were examined by scanning electron microscopy (SEM). The nitrogen adsorption equilibrium. isotherms were obtained using a QUADRASORB EVO analyzer measured at 77 K. All samples were degassed at 353 K for 4 h under vacuum before all porosity measurements. The specific surface area (S_{BET}) was determined by the Brunauer–Emmett–Teller (BET) theory, considering the molecular cross-sectional area of N2 at 77 K to be 0.162 nm^2. Pore size distribution and pore volume were calculated using the nonlocal density functional theory (NLDFT) with the carbon slit pore model. RAMAN spectra were obtained using a HORIBA LabRAM HR Evolution at room temperature with a laser source of 514 nm. Crystallographic properties of all samples were investigated by X-ray diffraction using an X-ray diffractometer D8 Advance operating at 40kV and recorded and 40 mA using Ni-filtered Cu Kα radiation (k = 0.15406 nm). Data was recorded in the 2θ range of 5° and 80° at a scanning rate of 1.5°/min with a step size of 0.02°. XPS was performed using a Thermo K-Alpha X-ray Photoelectron Spectrometer system using a monochromatic Al Ka x-ray source (*ca.* 1687 eV). The analyser's pass energy was set to 20 eV allowing for an energy resolution of 0.1eV. CasaXPS® was used to process the data. The binding energy scale was calibrated from the C 1s main peak of adventitious carbon at 285,0 eV (C-C/C-H). Scofield photoionization cross sections (corrected for the instrument transmission function and for the differences of analysis depths between elements) were used to calculate composition tables.[2]

Transmission electron microscopy samples were prepared by crushing the powder with ethanol and the small crystallites in suspension were deposited on a holey carbon film, supported by a

copper grid. The electron diffraction and the high-resolution electron microscopy were performed with a JEOL 2100F electron microscope equipped with a tilting and rotating goniometer (200 kV and point resolution of 1.8 Å) and coupled with EDX analysis (Oxford).

To investigate the materials' electrochemical properties, electrodes (A-MnO_2 and α-MnO_2) were prepared by mixing 75 wt% active material, 15 wt% carbon black and 10 wt% polytetrafluoroethylene (PTFE). The prepared paste was then kneaded into a paper-like form and dried at 60°C for 12 hours, before being pressed at ten tones on a 10 mm diameter stainless steel round mesh. The resulting electrodes had an active material loading above 2.5 mg.cm^{-2}. A zinc foil of 0.25 mm thickness was cut into a 10 mm diameter disc to be used as anode for the aqueous zinc-MnO_2 battery.

Electrochemical testing was undertaken using a Biologic VMP. CV and GCD tests were conducted in a potential window between 0.8 and 1.8 V.
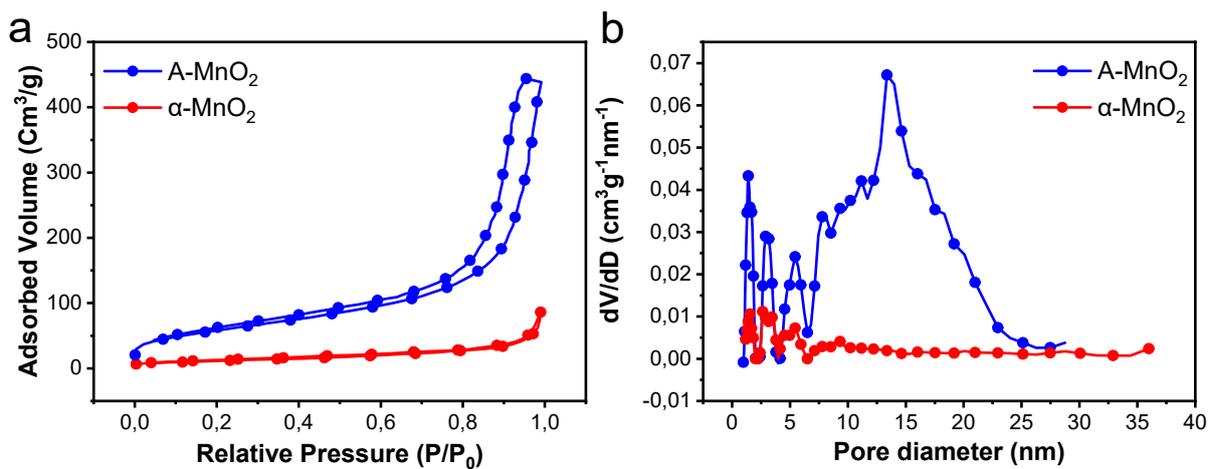
Figure S2: Sorption isotherms and pore size distribution of A-MnO$_2$ and α-MnO$_2$
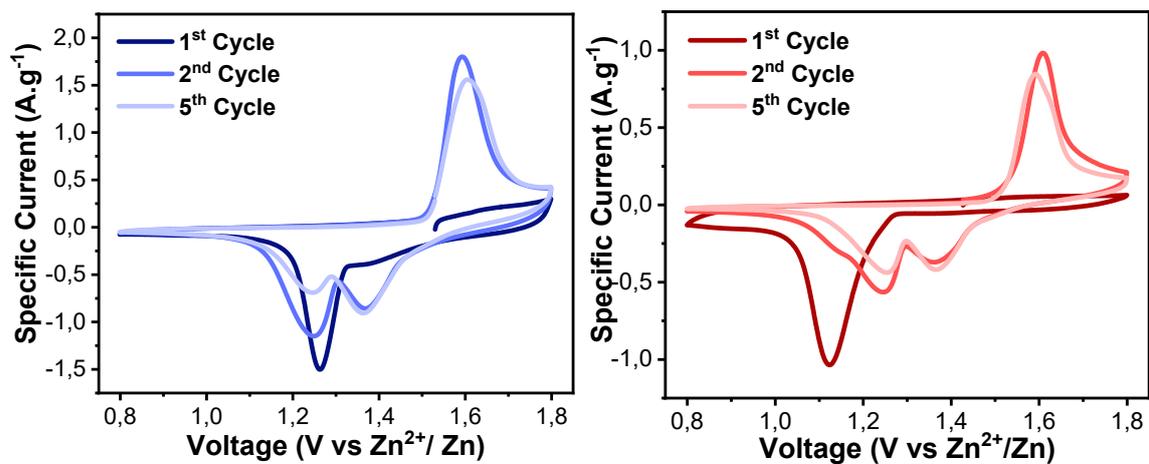
Figure S3: CV curves of A-MnO$_2$ (Blue) and α-MnO$_2$ (Red) at 0.3 mV.s^{-1}
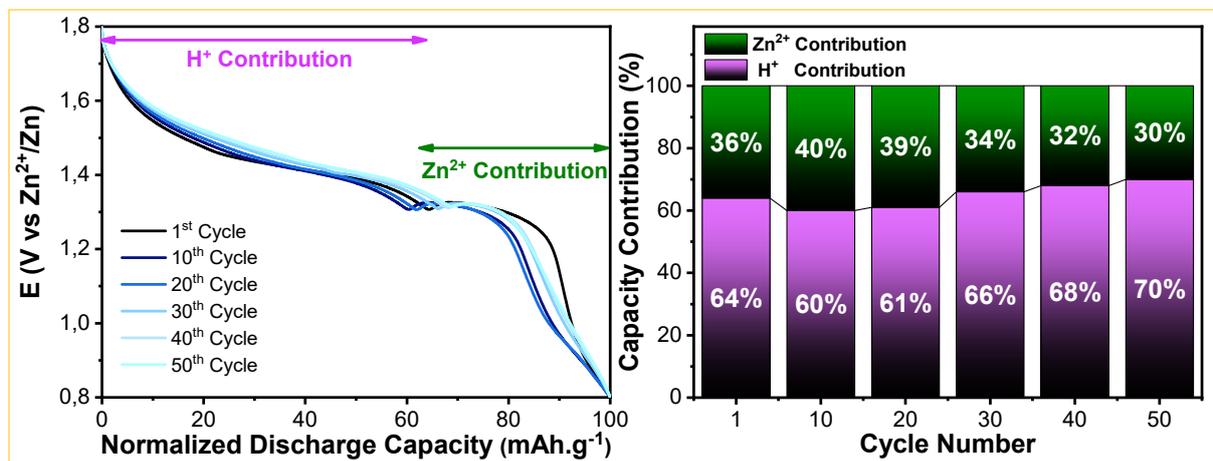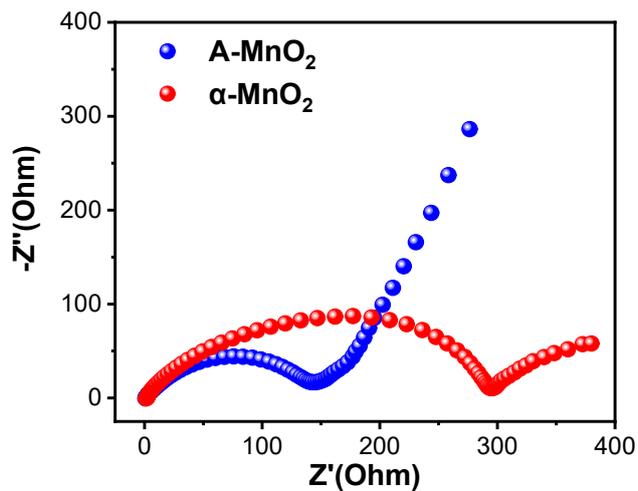
Figure S4: Nyquist plot of A-MnO$_2$ and α-MnO$_2$ at open circuit voltage

Figure S5: a) Normalized GCD patterns after long-term cycling of A-MnO$_2$ at 100 mA.g^{-1}, b)

Capacity contribution of A-MnO$_2$ after-long term cycling

Table S1: XPS composition table obtained for A-MnO$_2$

Core Peak	Mn 2p		O 1s			C 1s		
component	Mn^{3+}	Mn^{4+}	O-Mn	O$^-$	O-C	C-C,C-H	C-O	C=O
Binding Energy (eV)	641.3	642.2	529.8	531.4	532.8	285.0	286.2	288.6
Atomic %	13.6	7.4	34.6	15.1	0.9	21.7	1.8	5.0
Total Atomic %	21.0		50.6			28.5		

Table S2: XPS composition table obtained for ☐-MnO$_2$

Core Peak	Mn 2p		O 1s			C 1s		
component	Mn^{3+}	Mn^{4+}	O-Mn	O$^-$	O-C	C-C,C-H	C-O	C=O
Binding Energy (eV)	641.3	642.1	529.6	531.4	532.8	285.0	286.3	288.6
Atomic %	6.3	5.1	21.3	8.0	4.8	46.0	5.9	2.6
Total Atomic %	11.4		34.1			54.5		

References

1. Xiong T, Yu ZG, Wu H, et al. Defect Engineering of Oxygen-Deficient Manganese Oxide to Achieve High-Performing Aqueous Zinc Ion Battery. *Advanced Energy Materials*. 2019;9(14):1803815. doi:10.1002/aenm.201803815

2. Scofield JH. Hartree-Slater subshell photoionization cross-sections at 1254 and 1487 eV. *Journal of Electron Spectroscopy and Related Phenomena*. 1976;8(2):129-137. doi:10.1016/0368-2048(76)80015-1